Kashaev, N.; Ventzke, V.; Riekehr, S.; Dorn, F.; Horstmann, M.:

Assessment of alternative joining techniques for Ti–6Al–4V/CFRP hybrid joints regarding tensile and fatigue strength

In: Materials and Design (2015) Elsevier

DOI: 10.1016/j.matdes.2015.04.051

Assessment of alternative joining techniques for Ti-6Al-4V/CFRP hybrid joints regarding tensile and fatigue strength

Nikolai Kashaev, Volker Ventzke, Stefan Riekehr, Falk Dorn,
Manfred Horstmann

Institute of Materials Research, Materials Mechanics,
Helmholtz-Zentrum Geesthacht,
Max-Planck-Str. 1, 21502 Geesthacht, Germany
Contact: nikolai.kashaev@hzg.de

Highlights:

- Nd:YAG laser riveting of Ti-6Al-4V/CFRP lap joint was successfully realized
- Tensile strength is comparable to that of conventional riveted lap joints
- Fatigue strength of conventional riveted joint can be increased by adhesive bonding
- The effect of adhesive bonding is comparable to surface structuring of Ti-6Al-4V

Abstract:

CFRP and titanium joints are used in the aerospace industry. These materials are usually joined by titanium rivets which are inserted into holes drilled through both materials. Conventional riveted hybrid joints of CFRP and titanium parts fail under quasi static loading due to the uneven load distribution at the titanium rivets. Under cyclic loading, the fatigue failure occurs mainly in the titanium part because of the higher notch sensitivity. The aim of this work is the comparison of different joining concepts in terms of stiffness, strength and fatigue limit. First, laser riveting, here titanium pins are Nd:YAG laser beam welded to the Ti-6Al-4V parts. Second, conventional riveted hybrid joint is combined with adhesive bonding. Third, surface structuring of the Ti-6Al-4V parts is used to enhance friction in the riveted joint. Tensile and fatigue tests as well as fractographical examinations are performed to establish the process-property-performance relationship of the hybrid joints. Laser riveting leads to higher stiffness but equal strength, when compared to conventional riveted joints. Fatigue life is improved by the implementation of adhesive bonding and surface structuring.

Keywords: Laser riveting, adhesive bonding, surface structuring, Ti-6Al-4V, CFRP, fatigue strength

1. Introduction

New joining concepts and manufacturing technologies have been developed by the transportation industries to permit the use of lightweight structures to reduce carbon dioxide emissions and fuel consumption. To fulfil these goals, materials with a high strength-to-density-ratio, such as carbon fibre reinforced plastic (CFRP) and titanium are extensively used in modern aircraft structures [1-2]. The titanium alloy Ti-6Al-4V possesses high strength, sufficient ductility, low density and high corrosion resistance. Titanium is the only lightweight metal that can be directly attached to the CFRP structures without risking the development of corrosion defects [3].

The current overlap joining method for CFRP and titanium is still based on classical riveting technology. There are only few publications about alternative joining methods for titanium with CFRP available [4-12]. Adhesive bonding as direct alternative to riveting has been used for aircraft primary structures [4], 13]. However, the bonding of CFRP to titanium has still some obstacles to overcame due to the realization of proper and repeatable surface preparation of titanium and not controllable alteration of adhesive bonded joints [5,13]. Syassen et al. patented the method for joining of titanium alloys to CFRP by ultrasonic welding [6]. The ultrasonic welded bonds should have good properties with regard to the resistance to shear forces, corrosion resistance and durability and should be suitable for use in aircraft or spacecraft. Altmeyer et al. described the feasibility study of application the friction riveting for joining of grade 3 titanium with a short carbon fibre-reinforced polyether ether ketone [7]. The mechanical performance of the joints was only investigated in a tensile pull-out force test. Kocian et al. described hybrid structures of composites with integrated titanium layers, namely Ti-CF/PEEK laminates [8]. The hybrid structures can be adhesive bonded to titanium and composite and serve as a transition part between titanium and composite. Similar approach investigated by the researcher group named "Black-Silver" [9]. The purpose of realization

of hybrid structures by integration of titanium wires and titanium foils in the composites is to create the transition structures in fibre reinforced plastic aluminium compounds. However, the alternative joining techniques mentioned above were not investigated for joining of titanium with high strength duroplast CFRP materials that are typically used for primary airframe structures, where the behaviour of hybrid joints with regard to the residual strength and fatigue is of the great importance.

The objective of the research was the development of alternative joining methods to achieve improved strength and fatigue limit properties for the hybrid joint zone (HJZ) between titanium and CFRP. One approach is using laser beam welding (LBW) as a joining technology [10-12]. LBW (denoted also as laser riveting of Ti-6Al-4V/CFRP lap joint) process was developed and optimized in terms of the temperature distribution to avoid thermal damage of CFRP structure, the interface properties and the mechanical structure of the hybrid joint zone. Further approaches investigated in this study included the combination of an adhesive film, rivets and the use of a surface structured Ti-6Al-4V part to obtain a reinforcing pinning effect. Both a classical riveted joint and the modified hybrid joint zones were tested in standard tensile and fatigue tests to understand and compare their properties and failure mechanisms.

2. Experimental

2.1. Materials

A 2.5 mm thick Ti-6Al-4V sheet (grade 5, annealed) was lap joined to the CFRP material using different modified joint types to improve the load distribution compared with a conventional Ti-6Al-4V/CFRP rivet lap joint (reference joint). Additionally, the lap joint was used to assess changes to the tensile strength and fatigue life. The CFRP material consisted of M21E/34%/134/IMA-12K laminate with 20 ply layups of 25-mm x 200-mm plates that were 2.5 mm thick. The layup orientation is shown in Table 1. The layup with the highest ultimate tensile load for the three different orientations was chosen for use in these experiments. Titanium rivets (HI-LITE–EN6115 T3-4) with shaft diameters of 4.8 mm and with protruding heads were used for the reference joint. Seven different Ti-6Al-

4V/CFRP lap joint configurations were investigated. Three conventional HI-LITE rivets were used for a reference joint and were manually fastened to join a CFRP sheet to a Ti-6Al-4V plate (Fig. 1(a)).

Pins with diameters of 4.8 mm and 2.0 mm used for the laser riveting were fabricated from annealed Ti-6Al-4V titanium alloy rods. The heads of the pins were 9.0 mm and 4.0 mm in diameter, and the shafts were 4.8 mm and 2.0 mm in diameter, respectively.

Three types of laser riveted Ti-6Al-4V/CFRP lap joints were produced. The first type used 3 x 4.8-mm pins and was geometrically similar to a conventional lap joint. For other types of joints, the pin diameter, number and arrangement were modified to achieve a more even load distribution within the lap area. An array of 18 x 2.0-mm pins was implemented, which led to the second type of laser riveted Ti-6Al-4V/CFRP lap joints. The number of 2.0-mm pins (18) was set to realize an equivalent total area that is comparable to the reference joint with 3 x 4.8-mm rivets.

The CFRP material can be affected by the heat imparted into the materials during laser beam welding. A reference sample containing the same array of 18 x 2.0-mm pins was produced, whereas another sample used steel 42CrMo4 QT screws that were substituted for the Ti-6Al-4V pins. Steel 42CrMo4 QT screws were chosen because of their low cost and high shear strength compared to Ti-6Al-4V titanium alloy pins. Additionally, this choice was made to show that the heat input did not influence the mechanical behaviour of laser riveted Ti-6Al-4V/CFRP lap joints when subjected to static and cyclic load. The third type of specimen used a combination of 2 x 4.8-mm pins and 11 x 2.0-mm pins to additionally reinforce the lap joint.

An alternative approach for improving the load distribution was employing adhesive bonded Ti-6Al-4V/CFRP lap joints, which were drilled and fastened with HI-LITEs to create a reinforced bonded joint (adhesive bonded and joined with 3 x 4.8-mm conventional rivets). Cleaning and an abrasive treatment with a plastic blasting media of medium hardness were applied as a surface pre-treatment for CFRP parts before adhesive

bonding. Based on a study published by Kwakernaak et al. [13] a promising surface treatment consisted of cleaning, grit-blasting with an aluminium oxide and cleaning followed by a sol-gel treatment was chosen for Ti-6Al-4V parts. The bonding agent was made of the BR 127 primer and FM 73 epoxy. As shown in Fig. 11 the thickness of the adhesive layer was about 160 µm.

By way of substitution for adhesive bonding, the Ti-6Al-4V part was surface structured with a number of pyramids machined into the surface to obtain a reinforcing pinning effect (Fig. 1(b)). This approach is similar to the work of Ucsnik et al. [14] and Parkes et al. [15]. The surface structured Ti-6Al-4V parts were milled out of 4.0 mm Ti-6Al-4V parts. Curing of the pressed together Ti-6Al-4V and CFRP parts was accomplished in the autoclave. The cross section of Ti-6Al-4V/CFRP joints shows a good penetration of the pyramid into the CFRP material (Fig. 12). After curing the joints were drilled and fastened with HI-LITEs (surface structured and joined with 3 x 4.8-mm conventional rivets).

The overlapping area for all of the investigated titanium-CFRP specimens subjected to mechanical testing was 77 mm x 25 mm.

Table 1: Fibre orientations of the CFRP laminate layups.

Ply	1	2	3	4	5	6	7	8	9	10	11	12	13	14	15	16	17	18	19	20
Direction	45	-45	0	90	-45	45	0	0	90	0	0	90	0	0	45	-45	90	0	-45	45

(a)

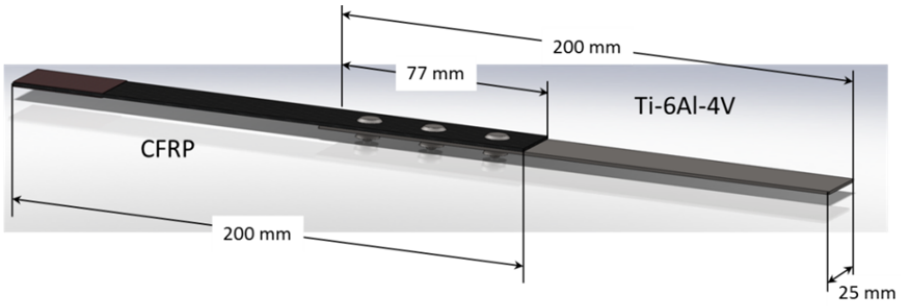

(b)

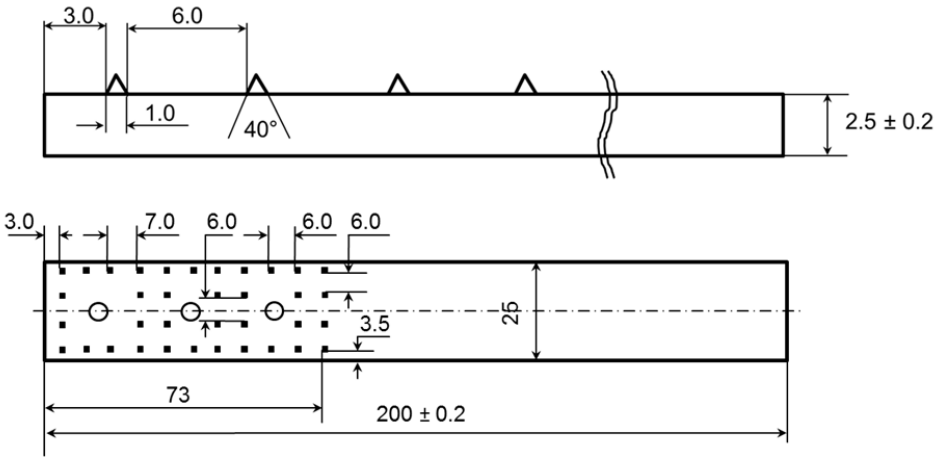

Fig. 1. (a) Model of a reference specimen used for tensile and fatigue testing with 3 x 4.8-mm rivets and (b) geometry of a surface structured Ti-6Al-4V part (all dimensions are in mm). The overlapping area of all of the investigated Ti-6Al-4V/CFRP specimens subjected to mechanical tests was 77 mm x 25 mm.

2.2 Laser riveting

The Ti-6Al-4V sheet and CFRP specimen were match-drilled together and dried cleaned afterward joining. The Ti-6Al-4V pins were cleaned in an alcohol solution prior to being placed in an ultrasonic bath and pushed through the holes of the plates with the head on the free surface of the CFRP plate. The parts were then clamped to the working table under the laser and welded via laser beam, as shown in Fig. 2(a). To ensure a tight joining via laser riveting, a pneumatic system was used to preload the CFRP part to the Ti-6Al-4V part. Standard pneumatic cylinders were used to realize a simple but effective clamping system: by a central argon pressure of 0.0, 1.5 and 8.0 bar applied to the cylinders a blank holder consisting of two parts was pressed downward on the CFRP part, keeping the CFRP and the Ti-6Al-5V part in a fixed position during the laser riveting

process. By the use of an argon driven pneumatic system no oxygen contamination could occur.

The Ti-6Al-4V sheet and CFRP specimen were lap joined by a continuous wave 3.3 kW Nd:YAG laser. A six-axis robot (KUKA KR 30 HA) was used to move the approximately 0.4 mm diameter laser beam. The specimens were fixed in an open box filled with Ar shielding gas to protect the Ti-6Al-4V weld bead from ambient air during the LBW process. Fig. 2(b) shows a macrograph of a laser riveted specimen with 11 x 2.0 mm pins and 2 x 4.8-mm pins.

The fixed laser riveting process parameters included the welding speed, Ar shielding gas and the clamping system. The parameters optimised for the laser riveting of the hybrid joints were the laser beam power, the structure preloading, the welding start and end points and the welding sequence.

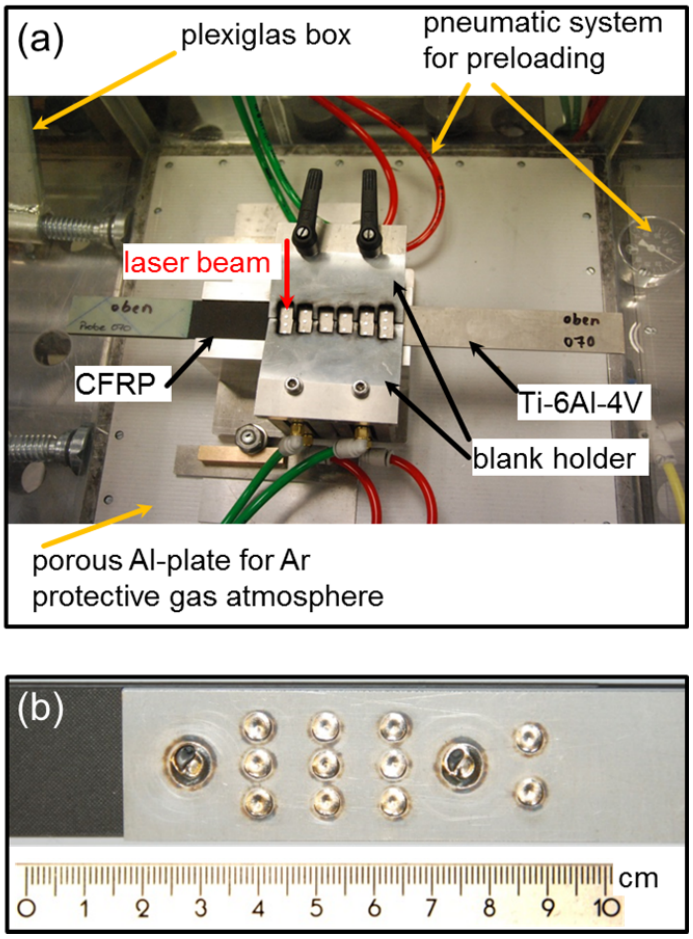

Fig. 2. (a) Experimental set-up used for the laser riveting process; (c) photograph of a laser riveted specimen with 11 x 2.0-mm pins and 2 x 4.8-mm pins.

2.3 Microstructural and Mechanical characterization

The microstructure of joints was studied using an optical microscope and SEM with electron back-scatter diffraction (EBSD). The EBSD measurements were performed for a specimen area of 125 µm x 125 µm, at 30 kV, a spot size of 3.5 nA, an emission current of 75 µA, a magnification of 750x, a working distance of 13 mm, a step size of 0.25µm, and a sample tilt of 70°. The orientation calculation was based on the GSHE method, assuming a triclinic sample symmetry. The microhardness profiles were obtained using an automated Vickers hardness testing machine.

The Ti-6Al-4V/CFRP lap joints were tested under monotonic shear loading conditions according to the DIN EN ISO 527-1 using a Zwick Roell RM100 machine equipped with

a 100 kN load cell. A Fiedler optoelectronic laser extensometer was used to measure the elongation. A servo-hydraulic 25 kN machine with an MTS control system was used for load-controlled fatigue tests at ambient temperature in air with a frequency of 40 Hz and an R-ratio of 0.1.

3. Results and discussion

3.1 Laser riveting of Ti-6Al-4V with CFRP

To identify the optimal laser beam power to weld the CFRP plate, Ti-6Al-4V sheet and Ti-6Al-4V pins, six specimens with 4.8-mm pins were welded using different laser powers followed by a metallographic investigation of their cross sections. Fig. 2(b) shows that the Ar gas atmosphere was stable during the laser riveting process. The Ti-6Al-4V side of the lap joint did not exhibit signs of coloured oxide layers. The power used for the laser riveting varied between 1500 and 2000 W. The welded area and the heat affected region of the welds were created using a laser power less than 1800 W that did not penetrate the CFRP plate. However, the slit of the same welds (Fig. 3(a)) is fairly long compared to the Ti-6Al-4V sheet thickness. It is clear that welding without a slit or a heat affected area on the CFRP (Fig. 3(b)) is not possible. The SEM observation of a CFRP heat affected zone (HAZ) showed that the higher heat input led to resin degeneration by vaporisation. Laid open fibres in the CFRP part were clearly seen by joints laser riveted by a laser power higher than 2000 W (Fig. 3(c)). Therefore, a compromise needs to be struck to realise a rivet weld that is of a satisfactory depth in the Ti-6Al-4V section and minimally affects the CFRP laminate. For the purposes of this study, a welding power of 1800 W was identified as the optimum value for welding the joints with 4.8-mm pins.

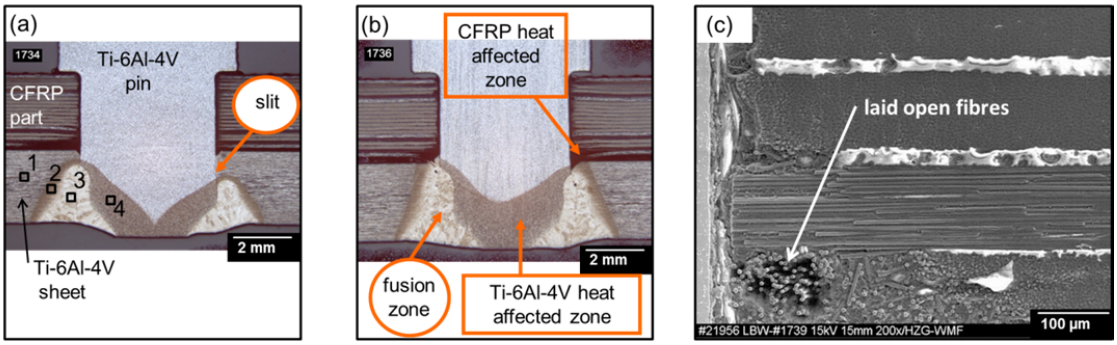

Fig. 3. Cross section of a 4.8-mm diameter laser rivet (a) welded by a laser power of 1800 W and (b) by a laser power of a 2000 W; (c) SEM image of a CFRP heat affected zone of a 4.8-mm diameter laser rivet, welded by a laser power of a 2000 W.

Fig. 4 shows the crystal orientation maps and inverse pole figures obtained from the different regions of the specimen welded by a laser power of 1800 W (cross-section of a 4.8-mm diameter laser rivet in Fig. 3(a)). The initial basal/transverse texture of the Ti-6Al-4V base material (BM) with a banded globular microstructure (Fig. 4(a)) was transformed into an acicular morphology with embedded globular grains in the HAZs (Fig. 4(b) and (d)) by the heat input during the laser riveting process and the subsequent cooling process. The centre of the fusion zone (FZ) consists of colonies of martensitic plates with pyramidal crystal directions (Fig. 4(c)). Distinct ⟨0 0 0 1⟩ crystal directions appeared within both HAZ regions (Fig. 4(b) and (d)), whereas the pole density of the ⟨1 0 -1 0⟩ crystal directions weakened relative to that of the BM. The differences in the microstructural morphology and crystallographic orientation would have corresponded to metallurgical notches. Further notches are present by geometrical imperfections of seam surface as well as by the slit between pin and sheet.

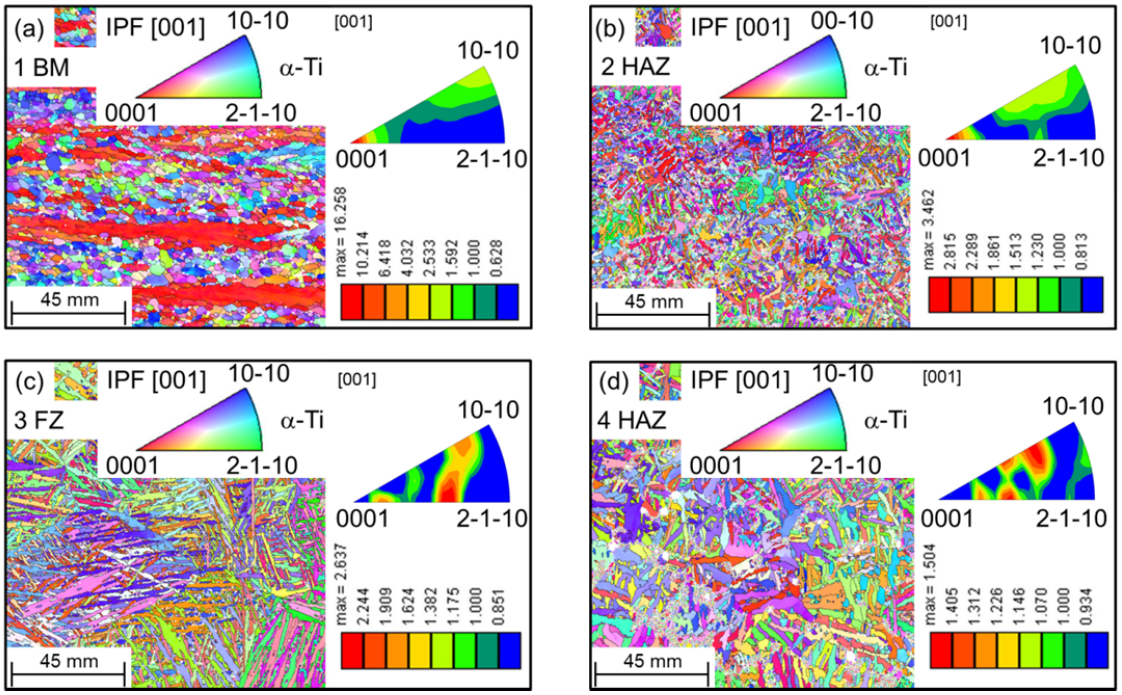

Fig. 4. Orientation maps and inverse pole figures obtained from the different regions of the specimen cross-section in Fig. 3(a): (a) BM (position 1, L_{max} = 22, H_{max} = 16.3 mrd); (b) HAZ (position 2, L_{max} = 22, H_{max} = 3.5 mrd); (c) FZ (position 3, L_{max} = 22, H_{max} = 2.6 mrd); (d) HAZ (position 4, L_{max} = 22, H_{max} = 1.5 mrd).

Laser power of 1700 W was found as a good compromise for the realization of 2.0-mm laser rivets with a satisfactory shape of the weld taking into account the minimization of the CFRP HAZ (Fig. 5(a)). The microhardness (Fig. 5(b)) increased inside the heat-affected zone from the Ti-6Al-4V pin BM to the FZ because of the presence of the martensitic plates (Fig. 4(c)). A higher microhardness of the welded pin in the region between the CFRP and Ti-6Al-4V parts would be preferable to improve the behaviour of the laser riveted joint with 18 x 2.0-mm pins under static and cyclic loading (Fig. 7(d) and Fig. 9(e)). However, the further increase of the welding zone thickness cannot be realised without damage of the CFRP part through the heat input during the laser riveting process. The notch effect as well the microhardness gradient (Fig. 5(b)) can amplify stress concentrations at the interfaces. It is well known that Ti–6Al–4Vexhibits an intense sensitivity to notches, which is reflected in its mechanical behavior under a cyclic load [19-20].

The Ti-6Al-4V is a good conductor of heat, and LBW is a process where a significant amount of heat is produced from the high power laser beam. The energy induced at the last welded pin is a combination of the laser beam power and the heat from the previous welds that is conducted to the area through the metal. This amount of energy results in welds with undesirable process voids. The melted resin can penetrate in the weld (the specimen on the left side in Fig. 10(b)) and thus the mechanical performance of the joint in the fatigue test will be reduced. The fracture is initiated at the end point of the weld. To address this, a different welding sequence was introduced to produce more uniform welds with a longer fatigue life expectancy (the specimen on the right side in Fig. 10(b)). As result of the experiments, a welding sequence as shown in Fig. 5(c) was identified for the 18 x 2.0-mm pins to achieve more uniform welds. 10-min time intervals every 3 welds were required to decrease the temperature of the Ti-6Al-4V part during welding.

To ensure a tight joining of the CFRP and Ti-6Al-4V parts via laser riveting, different preloading conditions of the parts to be joined were investigated. A series of samples were welded with the same laser power and clamped with a preload of 8.0, 1.5 and 0 bars. The fatigue life under the same, high loading conditions was then tested to determine if preloading was necessary. The best results with regard to the fatigue were achieved by a preload of 1.5 bar during laser riveting.

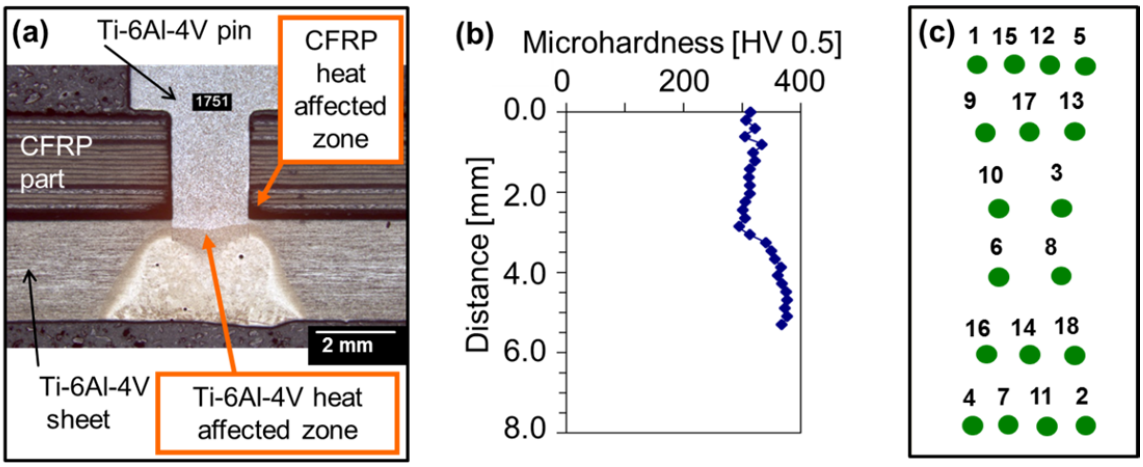

Fig. 5. (a) Cross section of a 2.0-mm diameter laser rivet welded by a laser power of 1700 W; (b) microhardness profile of the laser rivet and (c) welding sequence numbers for realization of 18 x 2.0-mm laser rivets with a 10 min time interval every 3 welds.

3.2 Tensile test results

The tensile test results are presented in Fig. 6 and Fig. 7. Table 2 shows the values of maximum load and stiffness determined in the tensile test. The stiffness of the specimens in kN / mm was calculated as the maximum load for the elastic region divided by the maximum elongation for the elastic region. The load-elongation (L-E)-curve for the reference joint (Fig. 6) shows typical behaviour for the riveted lap joint, as reported in [17]. The linear region is observed to an elongation of approximately 1.2 mm. At elongations greater than 1.2 mm, a well-documented type of bearing failure occurs in the riveted joints of the fibre reinforced plastic composites [16]. The area between 1.2 mm and 2.0 mm corresponds to the region between the loads of 30 kN, at which damage begins to occur, and 37 kN, at which failure is observed. Due to the advanced bearing failure at an elongation of 2.0 mm, corresponding rivet failure occurs. The failure always occurs at the rivet closest to the CFRP part due to the higher stiffness of CFRP compared to that of the Ti-6Al-4V (Fig. 7(a)).

The laser riveted lap joint with 3 x 4.8-mm pins shows a similar behaviour to the conventional riveted lap joint (Fig. 6). However, the laser riveted specimen has a higher initial stiffness up to an elongation of 0.3 mm. At an elongation of 0.3 mm, bearing

failure occurs, followed by shear failure of all of the pins between the CFRP and Ti-6Al-4V parts. The obtained failure load of 28 kN is lower than that of the conventional riveted lap joint (37 kN). A specimen with failured pins after the tensile test is represented in Fig. 7(b).

The specimens joined with 18 x 2.0-mm 42CrMo4 QT screws exhibit a linear region up to an elongation of 0.7 mm (Fig. 6). These specimens have a significantly smaller elongation area between the damage load of 27 kN at 0.7 mm and the failure load of 30 kN at 1.1 mm compared to the riveted reference specimen. The specimens joined with 18 x 2.0-mm 42CrMo4 QT screws exhibited shear fracture in all of the screws at the surface between the CFRP and Ti-6Al-4V parts (Fig. 7(c)). The bearing failure in the CFRP part was less pronounced. The higher initial stiffness of the Ti-6Al-4V/CFRP lap joint with 18 x 2.0-mm 42CrMo4 QT screws combined with a smaller elongation area between the damage load and the failure load and the shear failure of all of the screws indicated a more homogeneous load distribution between the screw array than was observed for the conventional riveted (reference) specimen.

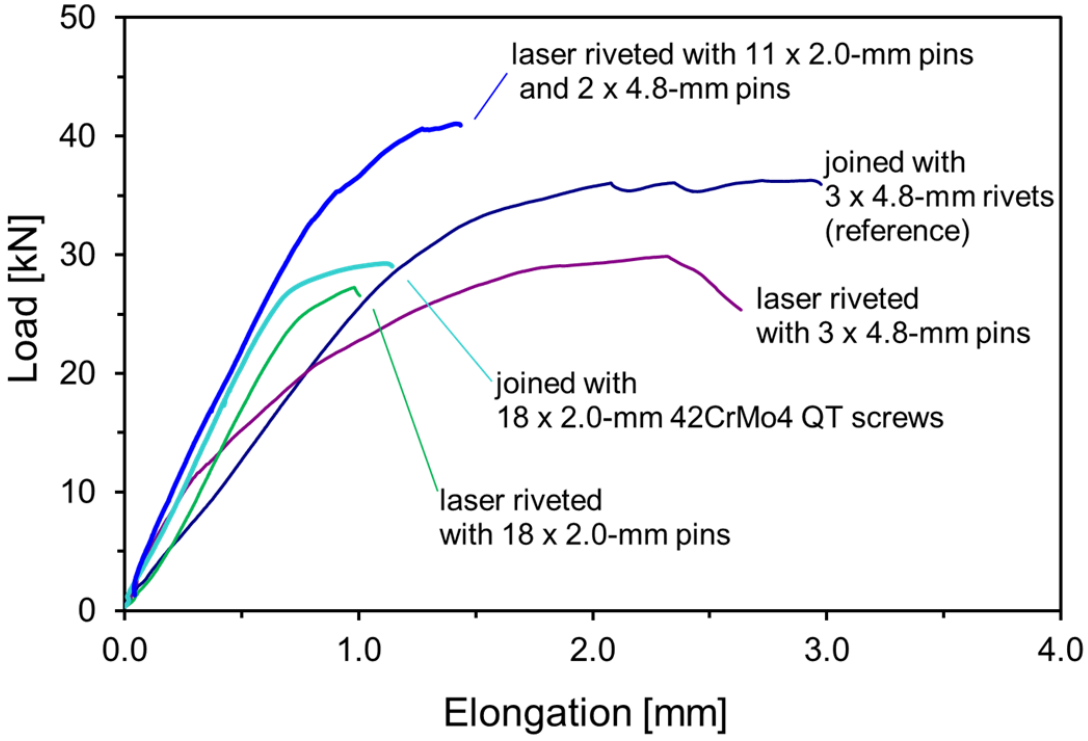

Fig. 6. Tensile test results. L-E-curves for one representative specimen of each joint.

Table 2: Maximum load and stiffness for the elastic region determined in the tensile test. Average values with standard deviations of three tested specimens

Joining method	Max. load [kN]	Stiffness [kN / mm]
Joined with 3 x 4.8-mm rivets (reference)	36.7 ± 0.9	24.8 ± 2.6
Joined with 18 x 2.0-mm 42CrMo4 QT screws	29.2 ± 0.1	38.3 ± 2.9
Laser riveted with 3 x 4.8-mm pins	29.1 ± 1.2	38.8 ± 2.6
Laser riveted with 18 x 2.0-mm pins	28.5 ± 1.8	36.3 ± 1.5
Laser riveted with 11 x 2.0-mm pins and 2 x 4.8-mm pins	40.3 ± 1.0	47.7 ± 1.3

The laser riveted Ti-6Al-4V/CFRP lap joint with 18 x 2.0-mm-pins shows a similar behaviour compare to the specimen joined with 18 x 2.0-mm 42CrMo4 QT screws (Fig. 6). However, this performance is inferior when compared to the Ti-6Al-4V/CFRP lap joint with 18 x 2.0-mm 42CrMo4 QT screws. The shear fracture of all of the laser-welded pins occurs at the Ti-6Al-4V HAZ/FZ interface between the CFRP and Ti-6Al-4V parts (Fig. 5(d)). This inferior performance can be explained by the reduced ductility associated with the unavoidable martensitic microstructure present in the HAZ/FZ-region.

The results obtained from the laser riveted lap joints with 18 x 2.0-mm pins as well as from the screwed lap joints indicate an improved load distribution within the lap zone compared to the reference specimen (Fig. 6). However, the shear strength of these specimens is less than was observed for the reference specimen with 4.8-mm rivets. Therefore, the influence of reinforcement of the laser riveted specimen using 2.0-mm pins with 2 additional 4.8-mm pins was investigated. The laser riveted specimens with 2 x 4.8-mm pins and 11 x 2.0-mm pins exhibit the highest initial stiffness and the best performance in the tensile test (Table 2). The implementation of the Ti-6Al-4V/CFRP lap joint with 2 x 4.8-mm pins and 11 x 2.0-mm pins does not increase the weight. The weight of the conventional lap joint is 7.8 g (weight of 3 Ti-6Al-4V rivets) and 7.3 g

(weight of all of the Ti-6Al-4V pins) in case of Ti-6Al-4V/CFRP lap joint with 2 x 4.8-mm pins and 11 x 2.0-mm pins, respectively.

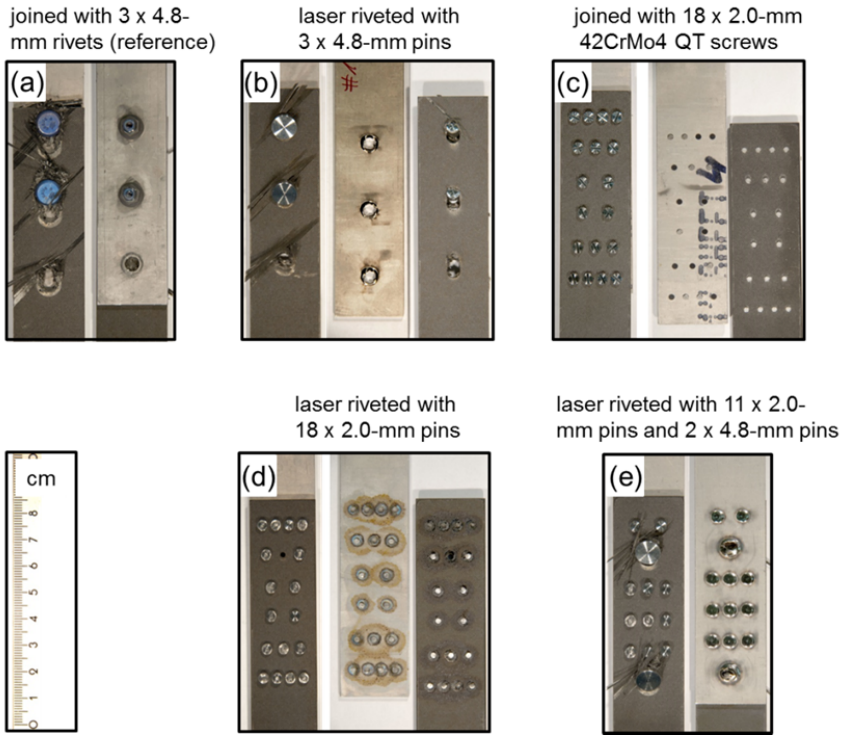

Fig. 7. Photographs of the specimens after the tensile test.

3.3 Fatigue test results

The load-lifetime (L–N) curves for the different Ti-6Al-4V lap joints are illustrated in Fig. 8. Fig. 9 shows photographs of fractured specimens after the fatigue tests. The fatigue strength of laser riveted Ti-6Al-4V/CFRP lap joint with 3 x 4.8-mm pins and 18 x 2.0-mm pins is essentially lower than the conventional riveted lap joint. For the conventional riveted lap joint, failure always occurred in the Ti-6Al-4V part at the rivet close to the CFRP part (Fig. 9(a), and Fig. 10(a)). The fracture was initiated at the hole around the rivet where the stresses were concentrated due to the tightening torque.

Fracture in the laser riveted Ti-6Al-4V/CFRP lap joint with 3 x 4.8-mm pins (appropriate welding sequence) always occurred in the HAZ between the Ti-6Al-4V pin and the Ti-6Al-4V BM (Fig. 9(b) and the specimen on the right side in Fig. 10(b)). The reason for

this fracture behaviour is the slit (Fig. 3(a)) that cannot be completely eliminated so as to minimise the HAZ in the CFRP part. A further reason is the HAZ between the Ti-6Al-4V pin and Ti-6Al-4V BM, which was located within the shear stress area. In [20], it was reported that the HAZ exhibited a martensitic microstructure adjacent to the FZ and may act as a metallurgical notch (Fig. 4). Moreover, the fatigue failure was caused by geometric imperfections in the welding seam. The Ti-6Al-4V/CFRP lap joint with 18 x 2.0-mm 42CrMo4 QT screws is geometrically similar to the laser riveted Ti-6Al-4V/CFRP lap joint with 18 x 2.0-mm pins when considering the pin and screw distribution. A comparison between these two specimens shows that the generation of geometric and metallurgical notches led to a degradation in the fatigue strength and the lifetime.

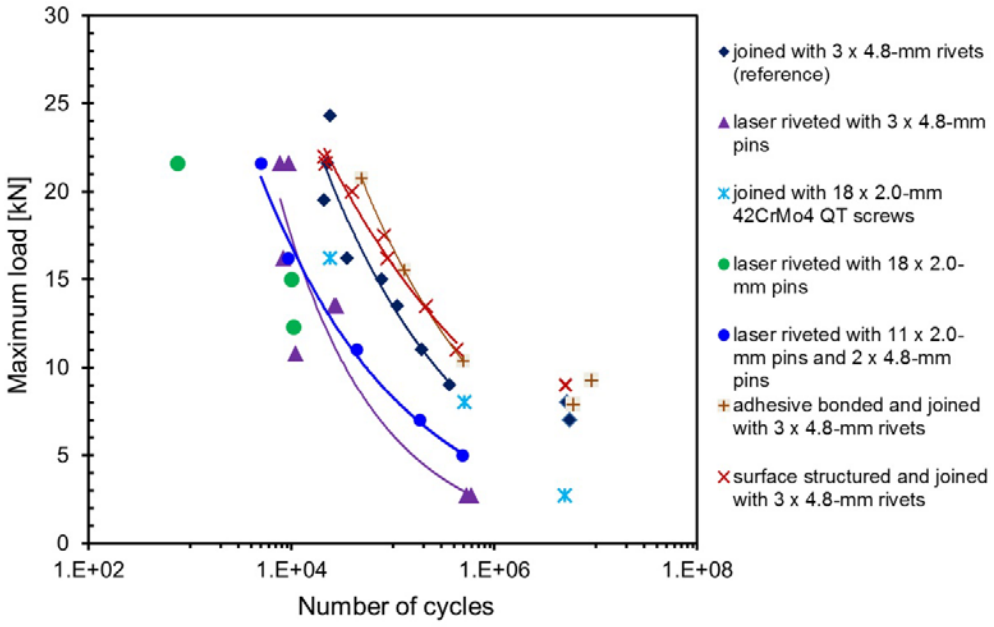

Fig. 8. Fatigue test results.

Compared to the conventionally riveted lap joint, the Ti-6Al-4V/CFRP lap joint with 18 x 2.0-mm 42CrMo4 QT screws exhibits a good fatigue performance in the low cycle fatigue range up to $1 \cdot 10^6$ cycles and inferior fatigue performance in the high cycle fatigue range (greater than $1 \cdot 10^6$ cycles). The fracture in the Ti-6Al-4V sheet occurs at a screw in the screw-draw close to the CFRP plate (Fig. 9(c)). However, the fracture

behaviour is similar to the laser riveted Ti-6Al-4V/CFRP lap joint containing 18 x 2.0-mm pins (Fig. 9(c) and (e)) due to the reduction of the pin diameter from 4.8 mm to 2.0 mm.

For the laser riveted Ti-6Al-4V/CFRP lap joint with 18 x 2.0-mm pins, the 2.0-mm pins were sheared exactly at the HAZ between the Ti-6Al-4V pin and Ti-6Al-4V BM (Fig. 8(e)). The Ti-6Al-4V plate and the CFRP plate were not damaged. The shearing of all the pins indicates that the weakest area exists between the plates in boundary region between the HAZ and FZ, where the so called geometric imperfections and metallurgical notch is present. These results are similar to those observed in case of Ti-6Al-4V fatigue specimen with laser beam welded butt joint [20].

The laser riveted specimens with 11 x 2.0-mm pins and 2 x 4.8-mm pins show slightly improved fatigue behaviour compared to the specimens that were laser riveted with 3 x 4.8-mm pins (Fig. 8). This lap joint type has exhibited fatigue fracture behaviour similar to that observed in a conventionally riveted lap joint (Fig. 8(a) and 8(f)). The reason for the inferior fatigue behaviour of the specimens laser riveted with 11 x 2.0-mm pins and 2 x 4.8-mm pins despite very good performance in the tensile test (Fig. 6) is the high notch sensitivity of the Ti-6Al-4V [19]. The welded specimens with pins have both geometric notches (slit (Fig. 3(a))) and metallurgical notches at the HAZ/FZ boundary, which have a greater effect on the fatigue behaviour then the reinforcing and homogeneous load distribution. The reason for the metallurgical notch can be the differences in the microstructural morphology and crystallographic orientation in the heat affected zone of the Ti-6Al-4V and the Ti-6Al-4V BM [20].

The fabrication of adhesive bonded Ti-6Al-4V/CFRP lap joints, which were additionally drilled and fastened with HI-LITEs to create a reinforced bonded joint, led to an essential improvement in the fatigue strength and lifetime. The riveted lap joint with a surface structured Ti-6Al-4V part exhibited similar fatigue behaviour to the adhesive bonded and riveted lap joint (Fig. 8, 9(a), 9(d) and 9(g)). Fig. 11(b) shows the presence of crack with in CFRP layers after the fatigue test. It indicates that shear stresses have led to the

interface debonding between the T-6Al-4V sheet and the adhesive layer. Fig. 12(b) clearly shows that a bend loading was active which resulted in a formation of a crack within the transition region between the Ti-6Al-4V surface and the pyramid. Both the adhesive layer and the surface structuring contributed to the reduction of the load stress at the rivet during the fatigue test. A higher static failure load and longer fatigue life of hybrid bolted and adhesive bonded composites joints than the only bolted joints was demonstrated by Fu and Mallic [18]. As the adhesive bonding of titanium with CFRP has still some obstacles to overcame due to the realization of proper and repeatable surface preparation of titanium and not controllable alteration of adhesive bonded joints, the surface structuring of Ti-6Al-4V in combination with riveting can be a good alternative to the adhesive bonding in combination with riveting.

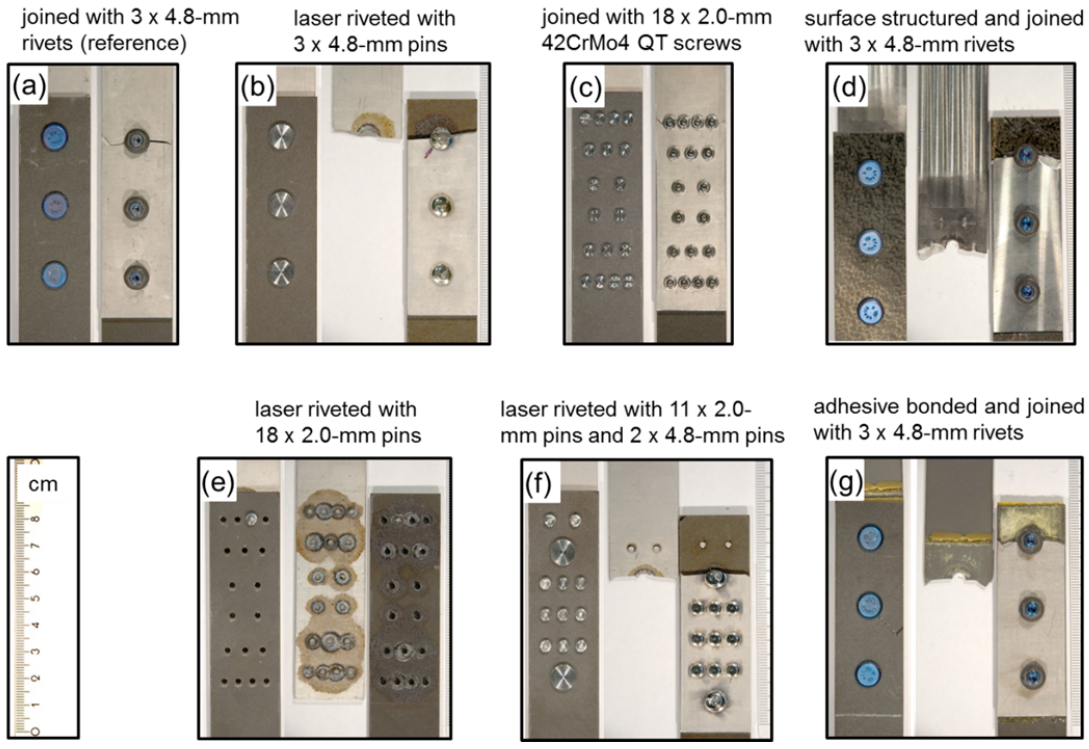

Fig. 9. Photographs of the specimens after the fatigue test.

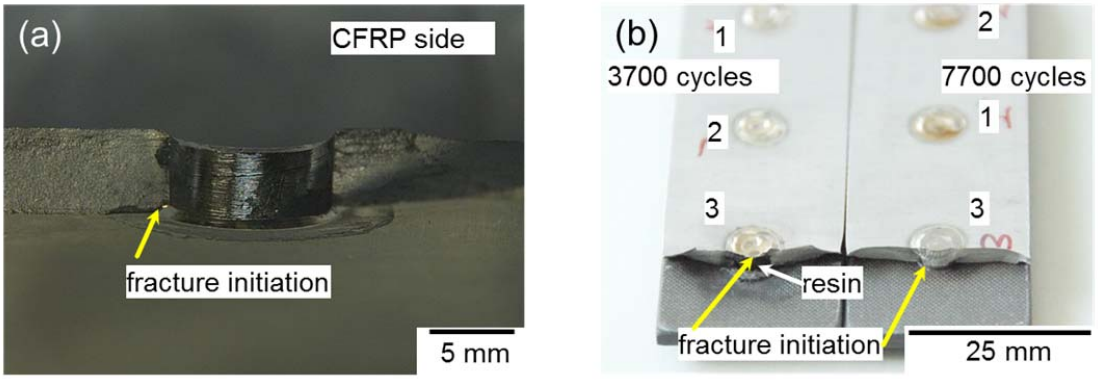

Fig. 10. (a) Photograph of Ti-6Al-4V part from a specimen joined with 3 x 4.8-mm rivets (standard) after the fatigue test; (b) photographs of two laser riveted specimens with 3 x 4.8-mm pins after the fatigue test with the welding sequence numbers: the specimen on the left side shows the resin in the welding zone and a reduced number of cycles until failure.

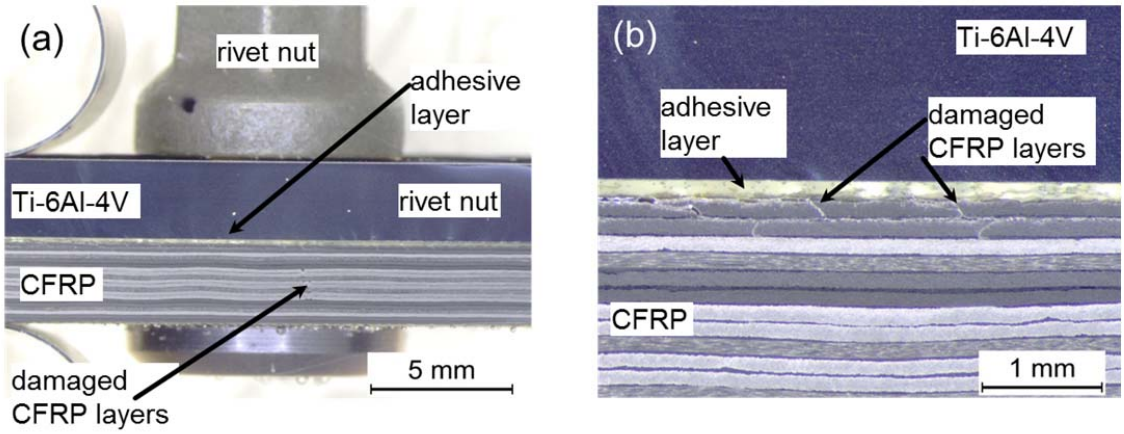

Fig. 11. (a) Photograph of a specimen adhesive bonded and joined with 3 x 4.8-mm rivets (standard) after the fatigue test (rivet number two) and (b) details of the macrograph as shown in (a).

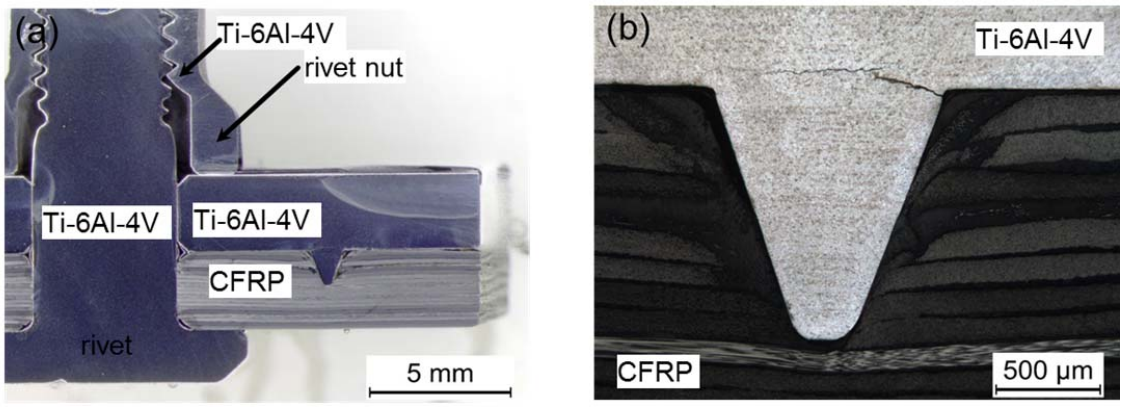

Fig. 12. (a) Photograph of a specimen surface structured and joined with 3 x 4.8-mm rivets (standard) after the fatigue test (rivet number two) and (b) details of the macrograph as shown in (a).

4. Conclusion

A conventionally riveted Ti-6Al-4V/CFRP lap joint can be improved by using a bonding agent made of the BR 127 primer and the FM 73 epoxy. Further improvements can be made by utilising geometric enhancements to the Ti-6Al-4V surface by machining pyramids into the surface to obtain a reinforcing pinning effect within the lap zone. The most essential result is that process conditions were identified which allow laser beam welding of Ti-6Al-4V and CFRP using Ti-6Al-4V pins without significant heat effect of CFRP structure. The tensile strength of the laser riveted Ti-6Al-4V/CFRP lap joint consisting of 2 x 4.8-mm pins and 11 x 2.0-mm pins is comparable to a conventional riveted Ti-6Al-4V/CFRP lap joint. However, the fatigue strength is lower because of the geometric and metallurgical notch effects in the Ti-6Al-4V. It was shown that different improved joining approaches for the hybrid joint zone can substitute the conventionally riveted Ti-6Al-4V/CFRP lap joint.

Acknowledgements

This work was carried out under the auspices of the OPTiSTRUCT project, which was funded by the German Ministry of Education and Research (BMBF) under contract no. 03CL05C. The financial support of the German BMBF is gratefully acknowledged. Additionally, the authors would like to thank Mr. R. Dinse and Mr. P. Haack from Helmholtz-Zentrum Geesthacht for their valuable technical support.

References

[1]. Hale J. Boeing 787 from the Ground Up. Boeing AERO Magazine 2006;4;17-23. http://www.boeing.com/commercial/aeromagazine/articles/qtr_4_06/AERO_Q406_article4.pdf.

[2]. Campbell K. Airbus to start manufacturing parts for new A350 XWB in late ’09. Creamer Media’s Engineering News 2009;May;11. http://www.engineeringnews.co.za/article/airbus-to-start-manufacturing-parts-for-new-a350-xwb-in-late-09-2009-05-11.

[3]. Murakami S, Ozaki K, Ono K, Itsumi Y. Effect of Alloying Elements on Machinability and Hot Workability of α-β Titanium Alloy Containing Fe and C. Kobelco Technology Review 2011;30;13-8. http://www.kobelco.co.jp/english/ktr/pdf/ktr_30/013-018.pdf

[4]. Higgins A. Adhesive bonding of aircraft structures. Int J Adhes Adhes 2000;20;367-376.

[5]. Molitor P, Barron V, Young T. Surface treatment of titanium for adhesive bonding to polymer composites: a review. Int J Adhes Adhes 2001;21;129-136.

[6]. Syassen F, Born J, Balle, F. Joining of titanium and titanium alloys to carbon fibres and carbon-fibre reinforced polymer components by ultrasonic welding. European Patent No EP 2 754 546 A1; 2014.

[7]. Altmeyer J, dos Santos JF, Amancio-Filho ST. Effect of the friction riveting process parameters on the joint formation and performance of Ti alloy/short-fibre reinforced polyether ether ketone joints. Mater Des 2014;60;164-76. http://dx.doi.org/10.1016/j.matdes.2014.03.042.

[8]. Kocian F, Hausmann J, Voggenreiter H. Hybride Werkstoffe und Strukturen für Luftstrahlantriebe. Konstruktion 2006;9;iw17-iw18.

[9]. Schimanski K, von Hehl A, Zoch HW. Failure behaviour of diffusion bonded transition structures for integral FRP-Aluminium compounds. Procedia Mater Sci 2013;2;189-96. http://dx.doi.org/10.1016/j.mspro.2013.02.023.

[10]. Kolossa S, Schnubel D, Riekehr S, Ventzke V, Rene D, Kashaev N. Method for the manufacture of a joint between a metal structure and a plastic composite structure. European Patent No 2 698 224 A1; 2014.

[11]. Kashaev N, Ventzke V, Kolossa S, Riekehr S, Horstmann M, Fomichev V, Arends S, Beck W. Development of joining concepts for titanium-CFRP parts. In: Greener Aviation 2014, Clean Sky Breakthroughs and Worldwide Status. Brussels, Belgium; 2014, www.greener-aviation2014.com.

[12]. Beck W, Kashaev N, Ventzke V, Reeder L (FormTech GmbH, Weyhe, Germany). Material and cost saving production processes for titanium and new design of the joining area CFRP-Ti as hybrid structure for improvement of load transfer and life time / OPTiSTRUCT. Final report to the project funded by the German BMBF under contract no. 03CL05C within the Aviation Cluster Hamburg Metropolitan Region; 2014 Feb.

[13]. Kwakernaak A, Hofstede J, Poulis J and Benedictus R. Improvements in bonding metals for aerospace and other applications. In: Chaturvedi MC, editor. Welding and joining of aerospace materials, Cambridge, UK: Woodhead Publishing Ltd; 2012, p. 235-87.

[14]. Ucsnik S, Scheerer M, Zaremba S, Pahr DH. Experimental investigation of a novel hybrid metal-composite joining technology. Compos Part A-Appl S 2010;41:369-74.

[15]. Parkes PN, Butler R, Meyer J, de Oliveira A. Static strength of metal-composite joints with penetrative reinforcement. Compos Struct 2014;118:250-6.

[16]. Hart-Smith LJ. Design and empirical analysis of bolted or riveted joints. In: Matthews FL, editor. Joining of fibre-reinforced plastics, Netherlands: Springer; 1987, p. 227-70.

[17]. Cooper C, Turvey GJ. Effects of joint geometry and bolt torque on the structural performance of single bolt tension in pultruded GRP sheet material. Compos Struct 1995;32:217-26. http://dx.doi.org/ 10.1016/0263-8223(95)00071-2.

[18]. Fu M, Mallick PK. Fatigue of hybrid (adhesive/bolted) joints in SRIM composites. Int J Adhes Adhes 2001;21;145-59. http://dx.doi.org/10.1016/S0143-7496(00)00047-6.

[19]. Peters M, Hemptenmacher J, Kumpfert J and Leyens C. Titanium and titanium alloys: structure, microstructure and properties (in German). In: Peters M, Leyens C, editors. Titan und Titanlegierungen, Weinheim, Germany: Wiley-VCH; 2002, p. 1-36.

[20]. Kashaev N, Ventzke V, Horstmann M, Riekehr S, Yashin G, Stutz L, Beck, W. Microstructure and Mechanical Properties of Laser Beam Welded Joints between Fine-Grained and Standard Ti-6Al-4V Sheets Subjected to Superplastic Forming. Adv Eng Mater 2015;17;374-82. http://dx.doi.org/10.1002/adem.201400202.